Simulating physical phenomena by quantum networks

R. Somma, G. Ortiz, J. E. Gubernatis, E. Knill, and R. Laflamme
Los Alamos National Laboratory, Los Alamos, New Mexico 87545
(Received 12 September 2001; published 9 April 2002)

Physical systems, characterized by an ensemble of interacting constituents, can be represented and studied by different algebras of operators (observables). For example, a fully polarized electronic system can be studied by means of the algebra generated by the usual fermionic creation and annihilation operators or by the algebra of Pauli (spin-1/2) operators. The Jordan-Wigner isomorphism gives the correspondence between the two algebras. As we previously noted, similar isomorphisms enable one to represent any physical system in a quantum computer. In this paper we evolve and exploit this fundamental observation to simulate generic physical phenomena by quantum networks. We give quantum circuits useful for the efficient evaluation of the physical properties (e.g., the spectrum of observables or relevant correlation functions) of an arbitrary system with Hamiltonian H.

DOI: 10.1103/PhysRevA.65.042323 PACS number(s): 03.67.−a, 05.30.−d

I. INTRODUCTION

A fundamental concept in quantum-information processing is the connection of a quantum computational model to a physical system by transformations of closed-operator algebras. The concept is a necessary one because in quantum mechanics each physical system is naturally associated with a language of operators (for example, quantum spin-1/2 operators) and thus to an algebra realizing this language (e.g., the Pauli spin algebra generated by a family of commuting quantum spin-1/2 operators). Any quantum system defined by an algebra of operators generated by a set of ''basic'' operators can be considered as a possible model of quantum computation [1]. The remarkable fact is that an arbitrary physical system is simulatable by another physical system (or quantum computer) whenever isomorphic mappings (embeddings) between the two operator algebras exists. In each such case, an important problem is to determine whether the simulation is efficient (polynomial resource overhead) in terms of the ''basic'' generators. For example, a nuclear spin (nuclear magnetic resonance NMR) quantum computer is modeled as a collection of quantum spin-1/2 objects and described by the Pauli algebra. It can simulate a system of ^{4}He atoms (with space discretized by a lattice) represented by the hard-core bosonic algebra and vice versa [1]. In this case, the simulation is efficient. Figure 1 summarizes this fundamental concept by giving a variety of proposed physical models for quantum computers and associated usable operator algebras. If one of these systems suffices as the universal model of quantum computing, the mappings between the operator algebras establish the equivalence of the other physical models to it. This is one's intuitive expectation and it has a well-established mathematical basis [3].

The mappings between algebras, between an algebra and a physical system, and between physical systems are necessary to simulate physical systems using a quantum computer fabricated on the basis of another system. However, their existence does not imply that the simulation is efficiently implementable. As we have previously discussed [1], efficient quantum computation involves more than having the ability to represent 2^N different items of classical information so that the algebra of N quantum bits (qubits) can be isomorphically represented and quantum parallelism can be exploited. It is also insufficient for the mapping between operator algebras to be easily and perhaps efficiently formalized symbolically. For example, the physical system consisting of one boson in 2^N modes is describable using the language of ''transition'' operators, represented by Pauli matrices on an N-qubit space, which move the boson from one mode to the other; however, the one-boson system is no more powerful than classical wave mechanics. This means that unless quantum computers are not as powerful as is believed, there is no efficient simulation of qubits by the one-boson system.

A quantum computer does, however, allow for the efficient simulation of some systems that are impractical on a classical computer. In our recent paper [1] we discussed how to simulate a system of spinless fermions by the ''standard model'' of a quantum computer, that is, the model expressed in the language and algebra of quantum spin-1/2 objects (Pauli algebra). We also discussed how to make certain physically interesting measurements. We demonstrated that the mapping between algebras is a step of polynomial complexity and gave procedures for initial state preparation, evolution, and certain measurements that scaled polynomially with complexity. The main focus of the paper, however, was to demonstrate that a particular problem for simulating fermions on a classical computer, called the dynamical-sign problem, does not exist on a quantum computer [4].

In this paper we continue to explore additional issues associated with efficient and effective simulations of physical systems on a quantum computer, issues that are independent of the particular experimental realization of the quantum computer. To be useful as a physics simulation device, a quantum computer must answer questions about physical properties associated with real physical systems. These questions are often concerned with the expectation values of specific measurements of a quantum state evolved from a specific initial state. Consequently, the initialization, evolution, and measurement processes must all be implementable with polynomial scaling [1]. Often this is difficult to do. Further, some classes of measurements, such as thermodynamic ones, still lack well-defined workable algorithms [6].

We seek to construct quantum-network models of such

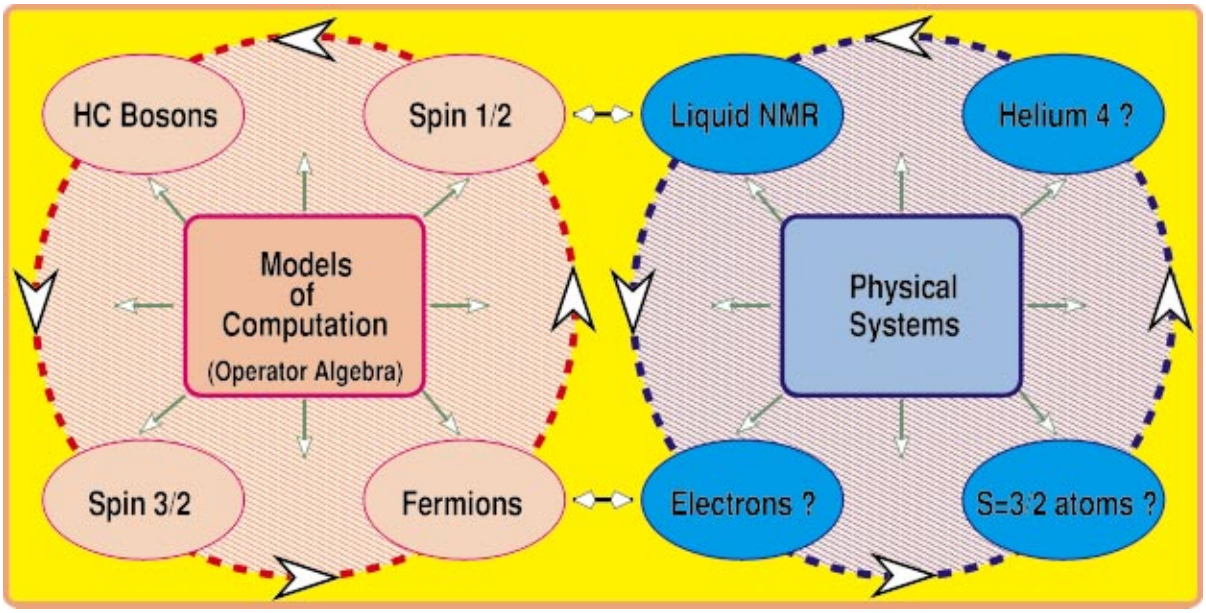

FIG. 1. (Color) Relationship between different models of computation (with their associated operator algebras) and different physical systems. Question marks refer to the present lack of a quantum computer device using the corresponding elementary physical components indicated in the box. Diamond-shaped arrows represent the natural connection between physical system and operator language, while arrows on the circle indicate the existence of isomorphisms of *-algebras, therefore, the corresponding simulation of one physical system by another. A wave function view of this relationship is given in [2].

measurements. Such networks are sets of elementary quantum gates to which we map our physical system. For simplicity, we discuss these issues relative to simulating a system of spin-1/2 fermions using the standard model of quantum computing [7]. Specifically we address issues discovered in our attempt to implement a (classical) simulator of a network-based quantum computer and to conduct a quantum computation on a physical system (NMR) with a small number of qubits. On a classical computer the number of qubits simulatable is limited by the exponential growth of the memory requirements. Physically, we can only process information experimentally with systems of a few qubits. Having the simulator permits a comparison between theory and experiments likely to be realizable in the near future. Overall, the main problems we address are how to reduce the number of qubits and quantum logic gates needed for the simulation of a particular physical phenomena, and how to increase the amount of physical information measurable by designing efficient quantum algorithms.

We have organized the paper in the following manner: In Sec. II we summarize the quantum-network representation of the standard model of quantum computation, discussing both one qubit and multiqubit circuits. Then we summarize the connection between the spin and fermion representations. In Sec. III, we first discuss the initialization, evolution, and measurement processes. In each case we define procedures simpler than those presented in our previous paper, greatly improving the efficiency with which they can be performed. Much expanded are the types of measurements now possible. For example, besides certain correlation functions, the spectrum of operators, including the energy operator, can now be obtained. Our application of this technology to a system of fermions on a lattice and the construction of a simulator is discussed in Sec. IV. The Hubbard model is used as an example. We conclude with a summary and a discussion of areas needing additional work. The appendixes contain technical points about the preparation of coherent and correlated states and the use of the discrete classical Fourier transformation.

II. QUANTUM-NETWORK REPRESENTATION OF PHYSICAL PHENOMENA

It is the formal connection between models of computation and physical systems described in the Introduction that allows one to simulate quantum phenomena with a quantum computer. Simulation is realized through a quantum algorithm that consists of unitary operations and measurements. One of the objectives is to accomplish simulation efficiently, i.e., with polynomial complexity. The hope is that quantum simulation is ''more'' efficient (less resources) than classical simulation and there are examples that support such hope [1]. In the following sections we summarize the main concepts in the representation of physical phenomena by quantum networks.

A. Standard model of quantum computation

In the standard model of quantum computation, the quantum bit, or *qubit*, is the fundamental unit. A qubit's state $|a\rangle = a|0\rangle + b|1\rangle (|a|^2 + |b|^2 = 1)$ is a linear combination of the states $|0\rangle$ and $|1\rangle$ (e.g., a spin 1/2 with $|0\rangle = |\uparrow\rangle$, $|1\rangle = |\downarrow\rangle$).

Assigned to each qubit are the identity matrix $\mathbb{1}$ and the Pauli matrices σ_x, σ_y, and σ_z, or equivalently $\mathbb{1}$, $\sigma_\pm = \frac{1}{2}(\sigma_x \pm i\sigma_y)$, and σ_z [8]. For a system of n qubits, the

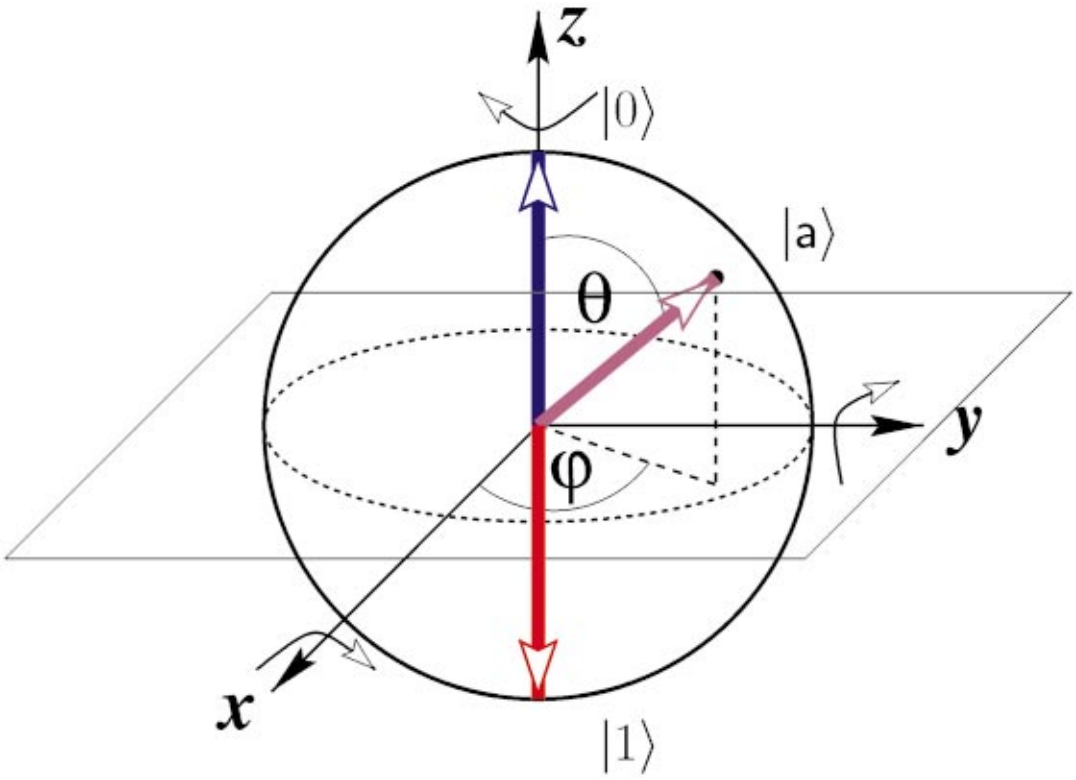

FIG. 2. (Color) Bloch-sphere representation of a one-qubit state parametrized as $|a\rangle=\cos(\theta/2)|0\rangle+e^{i\varphi}\sin(\theta/2)|1\rangle$. The curved arrows indicate the sign of rotation of $e^{i(t/2)\sigma_\mu}=R_\mu(-t)$ about the particular axis μ. Our (arrow) color convention is $|0\rangle\rightarrow$ blue, $|1\rangle\rightarrow$ red, other linear combinations $\rightarrow$ magenta.

mathematical representation of the standard model of quantum computing is defined by a closed *-algebra (Pauli algebra) generated by the operators $\sigma_\mu^j(\mu=x,y,\text{ or }z)$ that act on the jth qubit,

$$\sigma_\mu^j=\overbrace{\mathbb{1}\otimes\mathbb{1}\otimes\cdots\otimes\underbrace{\sigma_\mu}_{j\text{th factor}}\otimes\cdots\otimes\mathbb{1}}^{n\text{ factors}},$$

where $\otimes$ represents a Kronecker product. The resulting commutation relations are

$$[\sigma_\mu^j,\sigma_\nu^j]_+=2\delta_{\mu\nu}, \tag{2.1}$$

$$[\sigma_\mu^j,\sigma_\nu^k]_-=2i\delta_{jk}\epsilon_{\mu\nu\lambda}\sigma_\lambda^j, \tag{2.2}$$

where $[A,B]_\pm=AB\pm BA$ and $\epsilon_{\mu\nu\lambda}$ is the totally antisymmetric Levi-Civita symbol. The time evolution of an n-qubit system is described by the unitary operator $\hat{U}(t)=e^{-iHt}$, where H represents the time-independent Hamiltonian of the system. In turn, $\hat{U}(t)$ is easily expressible in terms of the Pauli matrices σ_μ^j since they and their products form an operator basis of the algebra.

B. Quantum network

In a quantum network, any unitary operator U can be decomposed (up to a phase) as $U=\Pi_l U_l$, where U_l are either single-qubit rotations $R_\mu(\vartheta)=e^{-i(\vartheta/2)\sigma_\mu}$ by an angle ϑ about the μ axis in the n-qubit space or two-qubit interactions $R_{z^j,z^k}(\omega)=e^{i\omega\sigma_z^j\sigma_z^k}$ in the same space (ω is a real number) [9,10]. The one-qubit rotations [Fig. 3(a)] and two-qubit interactions [Fig. 3(b)] constitute the elementary gates [11] of the quantum computer in the network model. For instance, if the evolution $\hat{U}(t)=e^{-iHt}$ is due to the typical Hamiltonian

$$H=H_x+H_y=\overline{\alpha}\,\sigma_x^1\sigma_z^2\cdots\sigma_z^{j-1}\sigma_x^j+\overline{\beta}\,\sigma_y^1\sigma_z^2\cdots\sigma_z^{j-1}\sigma_y^j, \tag{2.3}$$

where $\overline{\alpha}$ and $\overline{\beta}$ are real numbers, we write $\hat{U}(t)$ as $e^{-iH_xt}e^{-iH_yt}$ because $[H_x,H_y]_-=0$. To decompose this into one- and two-qubit operations, we take the following steps. We first note that the unitary operator

$$U_1=e^{i(\pi/4)\sigma_y^1}=\frac{1}{\sqrt{2}}[\mathbb{1}+i\sigma_y^1] \tag{2.4}$$

takes $\sigma_z^1\rightarrow\sigma_x^1$, i.e., $U_1^\dagger\sigma_z^1U_1=\sigma_x^1$, so $U_1^\dagger e^{i\overline{\alpha}\sigma_z^1}U_1=e^{i\overline{\alpha}\sigma_x^1}$. Next we note that the operator

$$U_2=e^{i(\pi/4)\sigma_z^1\sigma_z^2}=\frac{1}{\sqrt{2}}[\mathbb{1}+i\sigma_z^1\sigma_z^2]$$

takes $\sigma_x^1\rightarrow\sigma_y^1\sigma_z^2$, so $U_2^\dagger e^{i\overline{\alpha}\sigma_x^1}U_2=e^{i\overline{\alpha}\sigma_y^1\sigma_z^2}$. Then we note that

$$U_3=e^{i(\pi/4)\sigma_z^1\sigma_z^3}$$

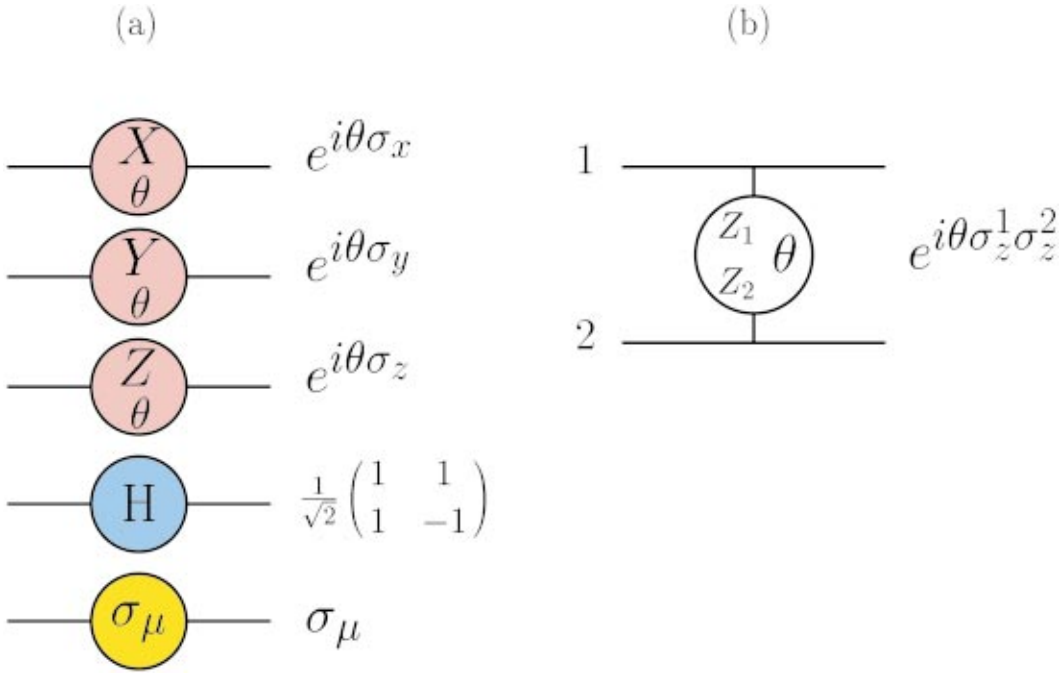

FIG. 3. (Color) (a) Some one-qubit elementary gates [notice that $e^{i\theta\sigma_\mu}=R_\mu(-2\theta)$ and $\sigma_\mu=ie^{-i(\pi/2)\sigma_\mu}$ is an $R_\mu(\pi)$ rotation up to a phase] and (b) a two-qubit elementary gate.

takes $\sigma_y^1\sigma_z^2\rightarrow-\sigma_x^1\sigma_z^2\sigma_z^3$. By successively similar steps we easily build the required string of operators: $\sigma_x^1\sigma_z^2\cdots\sigma_z^{j-1}\sigma_x^j$ and also $\exp(i\overline{\alpha}\sigma_x^1\sigma_z^2\cdots\sigma_z^{j-1}\sigma_x^j)$ (up to a global phase),

$$U_k^\dagger\cdots U_2^\dagger U_1^\dagger e^{i\overline{\alpha}\sigma_z^1}U_1U_2\cdots U_k=\exp(i\overline{\alpha}\sigma_x^1\sigma_z^2\cdots\sigma_z^{j-1}\sigma_x^j), \tag{2.5}$$

where the integer k scales polynomially with j (in this particular case the scaling is linear). In a similar way, we decompose the evolution e^{-iH_yt}. Multiplying both decompositions, we have the total decomposition of the evolution operator $\hat{U}(t)$. See [12,13] for complete treatments of these techniques.

1. Single-qubit circuits

The most general unitary operator U on a single qubit can be written as

$$U=e^{i\alpha}R_z(\beta)R_y(\gamma)R_z(\delta), \tag{2.6}$$

where α, β, γ, and δ are real numbers and $R_\mu(\vartheta)$ are single-qubit rotations. In Fig. 3(a) we show examples of several elementary one-qubit gates. In terms of the Pauli matrices, for instance, the Hadamard gate is $[H:|1(0)\rangle\rightarrow|+(-)\rangle=(|0\rangle\pm|1\rangle)/\sqrt{2}$, see Fig. 4(a)]

$$H=\frac{1}{\sqrt{2}}[\sigma_x+\sigma_z]=ie^{-i(\pi/2)\sigma_x}e^{-i(\pi/4)\sigma_y}. \tag{2.7}$$

In Fig. 4(b) we show the Bloch-sphere representation of the state $|+\rangle=(|0\rangle+|1\rangle)/\sqrt{2}$. The convention for quantum circuits is that each horizontal line represents the time evolution of a single qubit and the time axis of the evolution increases from left to right.

2. Multiple-qubit circuits

We now give examples of multiqubit operations. Consider the circuit shown in Fig. 5. This is a two-qubit controlled-NOT (CNOT) gate, which acts as follows:

$$\text{CNOT}:\begin{cases}|00\rangle\rightarrow|00\rangle,|01\rangle\rightarrow|01\rangle\\ |10\rangle\rightarrow|11\rangle,|11\rangle\rightarrow|10\rangle\end{cases}$$

Here, the first qubit is the control qubit (the controlled operation on its state $|1\rangle$ is represented by a solid circle in Fig. 5). We see that if the state of the first qubit is $|0\rangle$ nothing happens, but if the first qubit is in $|1\rangle$, then the state of the second qubit is flipped. The decomposition of the controlled-NOT operation into one- and two-qubits interaction is

$$\begin{aligned}CNOT:&e^{i\pi/4}e^{-i(\pi/4)\sigma_z^1}e^{-i(\pi/4)\sigma_x^2}e^{i(\pi/4)\sigma_z^1\sigma_x^2}\\ &=e^{i\pi/4}e^{-i(\pi/4)\sigma_z^1}e^{-i(\pi/4)\sigma_x^2}e^{i(\pi/4)\sigma_y^2}e^{-i(\pi/4)\sigma_z^1\sigma_z^2}e^{-i(\pi/4)\sigma_y^2}.\end{aligned} \tag{2.8}$$

From Eq. (2.8) we can see that a single controlled operation becomes a greater number (in this case five) of one- and two-qubits operations. In Fig. 5 we also show the circuit representing this decomposition, while in Fig. 6 we show the controlled-NOT gate applied to the state $|10\rangle$ in the Bloch-sphere representation.

A generalization of the controlled-NOT gate is the controlled-U (CU) gate, where U is a unitary operator acting on a multiqubit state $|\Psi_s\rangle$,

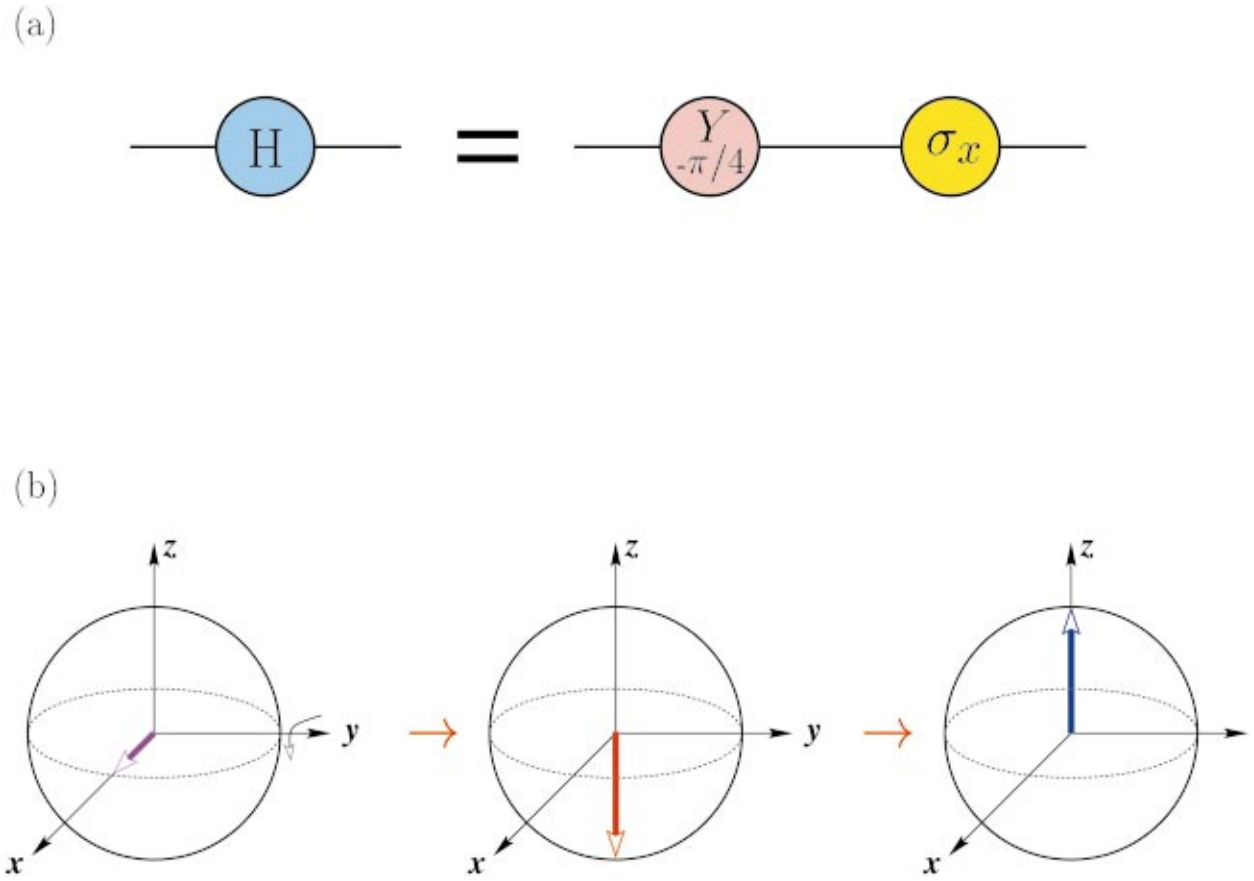

FIG. 4. (Color) (a) Hadamard-gate decomposition and (b) Bloch-sphere representation of a Hadamard gate applied to the state $|+\rangle$.

$$\begin{pmatrix} 1 & 0 & 0 & 0 \\ 0 & 1 & 0 & 0 \\ 0 & 0 & 0 & 1 \\ 0 & 0 & 1 & 0 \end{pmatrix}$$

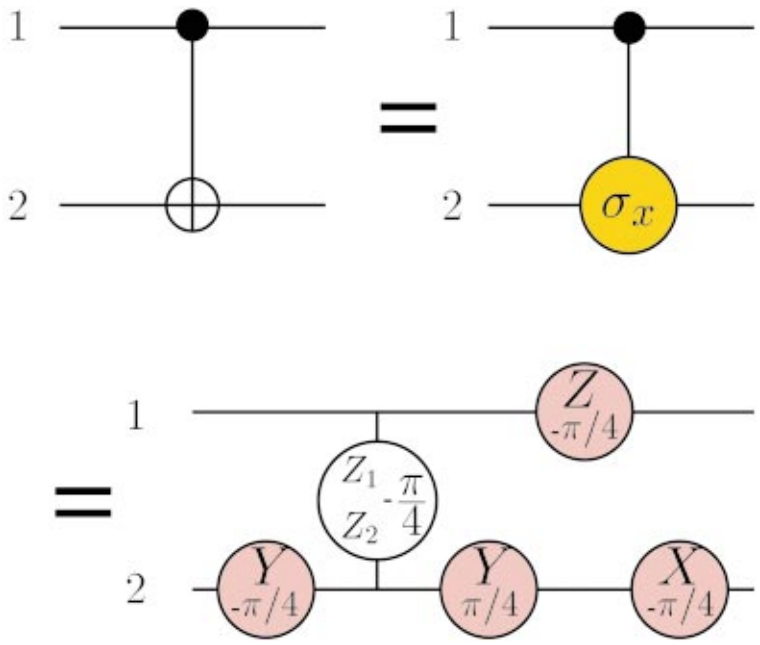

FIG. 5. (Color) Controlled-NOT gate decomposition and its matrix representation. The control qubit is 1. Note that the last circuit realizes the controlled-NOT matrix operation up to a global phase $e^{-i\pi/4}$.

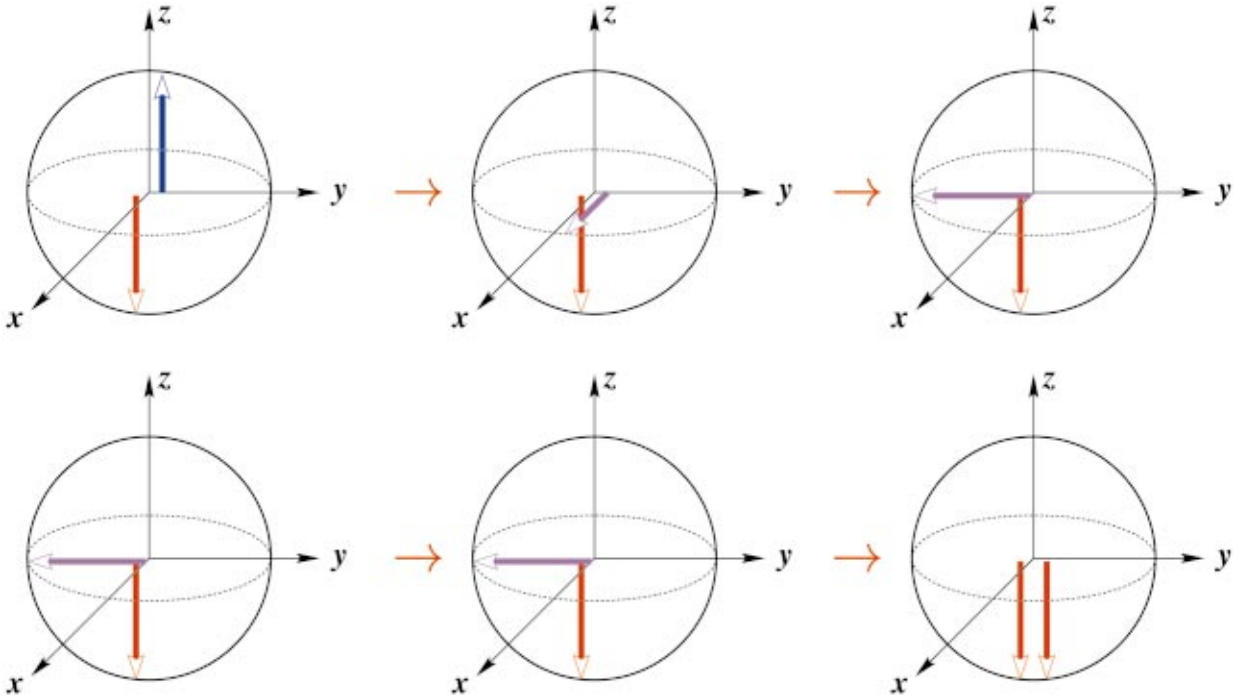

FIG. 6. (Color) Bloch-sphere representation of the state obtained by the controlled-NOT gate applied to the ''classical'' state $|10\rangle$. The sequence of elementary operations is the same as Fig. 5 (time flows from left to right with the lower row continuing the upper one). For each Bloch-sphere the two arrows indicate the states of the two qubits, with the left representing qubit 1.

$$CU:\begin{cases}|0\rangle_a\otimes|\Psi_s\rangle\rightarrow|0\rangle_a\otimes|\Psi_s\rangle\\ |1\rangle_a\otimes|\Psi_s\rangle\rightarrow|1\rangle_a\otimes[U|\Psi_s\rangle].\end{cases}$$

Mathematically, for $U(t)=e^{-i\hat{Q}t}$ ($\hat{Q}$ is Hermitian), the operational representation of the controlled-U gate is $U(t/2)U(t/2)^{-\sigma_z^a}$ $[U(t)^{-\sigma_z^a}=e^{i\hat{Q}\otimes\sigma_z^a t}]$, where a is the control qubit [Fig. 7(a)]. Similarly, one can use $|0\rangle_a$ as the control state to define the controlled-U' gate illustrated in Fig. 7(b).

C. Spin-fermion connection

To simulate fermionic systems with a quantum computer that uses the Pauli algebra, we first map the fermionic system

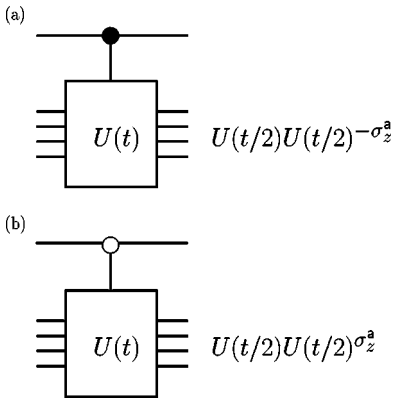

FIG. 7. (a) Controlled-U operation with the state of the control qubit a being $|1\rangle_a$ and (b) controlled-U' operation controlled with the state $|0\rangle_a$. (See text for notation.)

into the standard model [1,14]. The commutation relations for (spinless) fermionic operators a_j and $a_j^\dagger$ (the destruction and creation operators for mode j) are

$$[a_j^\dagger,a_k]_+=\delta_{jk},\quad [a_j^\dagger,a_k^\dagger]_+=0. \tag{2.9}$$

We map this set of operators to another set expressed in terms of the σ_μ^j's in the following way:

$$a_j\rightarrow\left(\prod_{l=1}^{j-1}-\sigma_z^l\right)\sigma_-^j=(-1)^{j-1}\sigma_z^1\sigma_z^2\cdots\sigma_z^{j-1}\sigma_-^j,$$

$$a_j^\dagger\rightarrow\left(\prod_{l=1}^{j-1}-\sigma_z^l\right)\sigma_+^j=(-1)^{j-1}\sigma_z^1\sigma_z^2\cdots\sigma_z^{j-1}\sigma_+^j.$$

The mapping just described (it indeed induces an isomorphism of *-algebras) is the famous Jordan-Wigner transformation [15]. Using this transformation, we can describe any fermionic unitary evolution in terms of spin operators and, therefore, simulate fermionic systems by a quantum computer. Although the mapping as given is for spinless fermions and for one-dimensional systems, it extends to higher spatial dimensions and to spin-1/2 fermions by remapping each ''mode'' label into a new label corresponding to ''modes'' in a one-dimensional chain. In other words, if we want to simulate spin-1/2 fermions in a finite $N_x\times N_y$ two-dimensional lattice, we map the label of the two-dimensional lattice to an integer number S, running from 1 to $2(N_x\times N_y)$. S identifies a mode in the new chain,

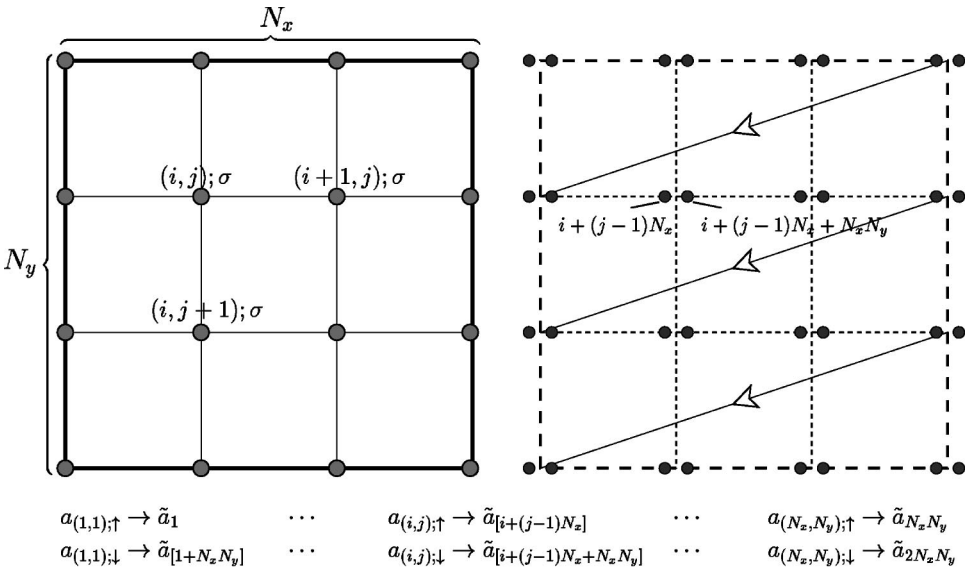

FIG. 8. Mapping used to connect the labels of a two-dimensional $N_x\times N_y$ lattice to the labels of a chain (i.e., a one-dimensional array of integer numbers).

$$a_{(j,k);\sigma}\to\tilde{a}_S\to\left(\prod_{l=1}^{S-1}-\sigma_z^l\right)\sigma_-^S=(-1)^{S-1}\sigma_z^1\sigma_z^2\cdots\sigma_z^{S-1}\sigma_-^S,$$

$$a_{(j,k);\sigma}^\dagger\to\tilde{a}_S^\dagger\to\left(\prod_{l=1}^{S-1}-\sigma_z^l\right)\sigma_+^S=(-1)^{S-1}\sigma_z^1\sigma_z^2\cdots\sigma_z^{S-1}\sigma_+^S, \tag{2.10}$$

where the $a_{(j,k);\sigma}$ and $a_{(j,k);\sigma}^\dagger$ are the fermionic spin-1/2 operators in the two-dimensional lattice for the mode (j,k) and for the z component of the spin $\sigma(\sigma=\pm\frac{1}{2})$, and $\tilde{a}_S$ and $\tilde{a}_S^\dagger$ are the spinless fermionic operators in the new chain. In our case, the modes are the sites and the label (j,k) identifies the X-Y position of this site $(j,k\in[1,N_{x,y}])$. The label $(j,k);\sigma$ maps into the label S (Fig. 8) via

$$S=j+(k-1)N_x+\left(\frac{1}{2}-\sigma\right)N_xN_y. \tag{2.11}$$

This is not the only possible mapping to a two-dimensional lattice using Pauli matrices [3,16,17], but it is very convenient for our simulation purposes.

III. QUANTUM-NETWORK SIMULATION OF A PHYSICAL SYSTEM

Like the simulation of a physical system on a classical computer, the simulation of a physical system on a quantum computer has three basic steps: the preparation of an initial state, the evolution of the initial state, and the measurement of the physical properties of the evolved state. We will consider each process in turn, but first we note that on a quantum computer there is another important consideration, namely, the relationship of the operator algebra natural to the physical system to the algebra of the quantum network. Fortunately, the mappings (i.e., isomorphisms) between arbitrary representations of Lie algebras are now known [3]. Section II C is just one example. To emphasize this point, the context of our discussion of the three steps will be the simulation of a system of spinless fermions by the standard model, which is representable physically as a system of quantum spin-1/2 objects.

A. Preparation of the initial state

The preparation of the initial state is important because the properties we want to measure (correlation functions, energy spectra, etc.) depend on it. As previously discussed [1], there is a way to prepare a fermionic initial state of a system with N_e spinless fermions and n single-particle modes j, created by the operators $a_j^\dagger$ (creation of a fermion in the mode j). In the most general case, the initial state is a linear combination of Slater determinants

$$|\Phi_\alpha\rangle=\prod_{j=1}^{N_e}b_j^\dagger|v\rangle, \tag{3.1}$$

described by the fermionic operators b_j and $b_j^\dagger$, which are related to the operators a_j and $a_j^\dagger$ via a canonical (unitary) transformation. Here $|v\rangle$ is the vacuum state (zero-particle state). To prepare $|\Phi_\alpha\rangle$ one can look for unitary transformations U_m such that

$$|\Phi_\alpha\rangle=e^{i\gamma}\prod_{m=1}^{N_e}U_m|v\rangle, \tag{3.2}$$

where γ is a phase factor. To perform these operations in the standard model we must express the U_m in terms of Pauli matrices using the Jordan-Wigner transformation. (We can do the mapping between the Pauli operators and the a_j operators or between the Pauli operators and the b_j operators. In the following we will assume the first mapping since this will simplify the evolution step.) One can choose $U_m=e^{-iH_mt}$ such that H_m is linear in the b_m and $b_m^\dagger$ operators [1]. We have to decompose the U_m into single-qubit rotations and two-qubit interactions $R_\mu(\vartheta)$ and $R_{z^j,z^k}(\omega)$. To do this, we first decompose the U_m into a products of operators linear

in b_m or $b_m^\dagger$; however, this decomposition does not conserve the number of particles. The situation appears complex.

Simplification occurs, however, by recalling the Thouless's theorem [18], which says that if

$$|\phi\rangle = \prod_{j=1}^{N_e} a_j^\dagger |v\rangle \tag{3.3}$$

and M is a $n\times n$ Hermitian matrix, then

$$|\Phi_\alpha\rangle = e^{i\vec{a}^\dagger M \vec{a}} |\phi\rangle, \tag{3.4}$$

where $\vec{a}^\dagger = (a_1^\dagger, \ldots, a_n^\dagger)$ and

$$\vec{b}^\dagger = e^{iM}\vec{a}^\dagger. \tag{3.5}$$

From Eq. (3.5) the operator e^{iM} (formally acting on the vector of $a_j^\dagger$'s) realizes the canonical transformation between a_j and b_j.

Thouless's theorem generalizes to quantum-spin systems via the Jordan-Wigner transformation. This theorem allows the preparation of an initial state by simply applying the unitary operator $e^{i\vec{a}^\dagger M \vec{a}}$ to a "boot-up" state polarized with each qubit being in the state $|0\rangle$ or $|1\rangle$. Indeed, for an arbitrary Lie operator algebra the general states prepared in this fashion are known as Perelomov-Gilmore coherent states [19].

The advantage of this theorem for preparing the initial state instead of the method previously described [1] is that the decomposition of the unitary operator $e^{i\vec{a}^\dagger M \vec{a}}$ can be done in steps, each using combinations of operators $a_j a_k^\dagger$ and, therefore, conserving the number of particles. Once the decomposition is done, we then write each operator in terms of the Pauli operators to build a quantum circuit in the standard model. (See Appendix A for a simple example.)

A single Slater determinant is a state of independent particles. That is, from the particle perspective, it is unentangled. Generically, solutions to interacting many-body problems are entangled (correlated) states, that is, a linear combination of many Slater determinants not expressible as a single Slater determinant. In particular, this is the case if the interactions are strong at short ranges. In quantum many-body physics, considerable experience and interest exists in developing simple approaches for generating several specific classes of correlated wave functions [18]. In Appendix A we illustrate procedures and recipes to prepare one such class of correlated (entangled) states, the so-called Jastrow states [18].

B. Evolution of initial state

The evolution of a quantum state is the second step in the realization of a quantum circuit. The goal is to decompose this evolution into the "elementary gates" $R_\mu(\vartheta)$ and $R_{zj,zk}(\omega)$. To do this for a time-independent Hamiltonian, we can write the evolution operator as $\hat{U}(t) = e^{-iHt}$, where $H = \Sigma_l H_l$ is a sum of individual Hamiltonians H_l. If the commutation relations $[H_l, H_{l'}]_- = 0$ hold for all l and l', then

$$\hat{U}(t) = \prod_l U_l(t) = \prod_l e^{-iH_l t}. \tag{3.6}$$

In this way, we can then decompose each $U_l(t)$ in terms of one- and two-qubit interactions using the method described in Sec. II B.

In general, the Hamiltonians H_l for different l do not commute and the decomposition in Eq. (3.6) cannot be used. Although we can, in principle, exactly decompose the operator $\hat{U}(t)$ into one- and two-qubit interactions [9,10], such a decomposition is usually very difficult. To avoid this problem, we decompose the evolution $\hat{U}(t) = \Pi_{j=1}^{\mathcal{M}} e^{-iH\Delta t}$ using the the first-order Trotter approximation ($t = \mathcal{M}\Delta t$),

$$\hat{U}(\Delta t) = e^{-iH\Delta t} = \exp\left(-i\sum_l H_l \Delta t\right) = \prod_l e^{-iH_l\Delta t} + \mathcal{O}((\Delta t)^2). \tag{3.7}$$

Then, for $\Delta t \to 0$, we can approximate the short-time evolution by $\hat{U}(\Delta t) \approx \Pi_l e^{-iH_l\Delta t}$. In general, each factor is easily written as one- and two-qubit operations (Sec. II B).

The disadvantage of this method is that approximating the operator $\hat{U}(t)$ with high accuracy might require Δt to be very small so that the number of steps $e^{-iH_l\Delta t}$ and hence the number of quantum gates required becomes very large. To mitigate this problem, we can use a higher-order Trotter decomposition. For example, if $H = K + V$, we then use the second-order Trotter approximation to decompose the evolution as $\hat{U}(t) = \Pi_{j=1}^{\mathcal{M}} e^{-iH\Delta t}$ with (second-order decomposition)

$$e^{-iH\Delta t} = e^{-iK\Delta t/2} e^{-iV\Delta t} e^{-iK\Delta t/2} + \mathcal{O}((\Delta t)^3) \tag{3.8}$$

$$= e^{-iV\Delta t/2} e^{-iK\Delta t} e^{-iV\Delta t/2} + \mathcal{O}((\Delta t)^3). \tag{3.9}$$

Other higher-order decompositions are available [20].

C. Measurement of physical quantities

1. One-ancilla qubit measurement processes

The last step is the measurement of the physical properties of the system that we want to study. Often we are interested in measurements of the form $\langle U^\dagger V\rangle$, where U and V are unitary operators [1]. Reference [1] gives a description of the type of correlation functions that are related to these measurements. Reference [21] gives an applications and variations of these techniques. Here, we simply give a brief description of how to perform such measurements.

First, we prepare the system in the initial state $|\Psi_0\rangle$ and adjoin to it one-ancilla (auxiliary) qubit a in the state $|+\rangle = (|0\rangle + |1\rangle)/\sqrt{2}$. This state is prepared by applying the unitary Hadamard gate to the state $|0\rangle$ (Fig. 4). Next, we make two controlled unitary evolutions using the CU and CU′ gates (Sec. II B 2). The first operation $\tilde{V}$ evolves the system by V if the ancilla is in the state $|1\rangle$: $\tilde{V} = |0\rangle\langle 0| \otimes \mathbb{1} + |1\rangle\langle 1| \otimes V$. The second one $\tilde{U}$ evolves the system by U if the

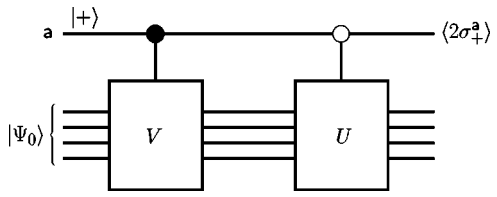

FIG. 9. Measurement of physical quantities using one extra (ancilla) qubit $|a\rangle$. In this case $\langle 2\sigma_+^a\rangle=\langle\Psi_0|U^\dagger V|\Psi_0\rangle$.

ancilla state is $|0\rangle$: $\tilde{U}=|0\rangle\langle 0|\otimes U+|1\rangle\langle 1|\otimes\mathbb{1}$. ($\tilde{V}$ and $\tilde{U}$ commute.) Once these evolutions are done, the expectation value of $2\sigma_+^a=\sigma_x^a+i\sigma_y^a$ gives the desired result $\langle U^\dagger V\rangle$. This quantum circuit is shown in Fig. 9. Note that the probabilistic nature of quantum measurements implies that the desired expectation value is obtained with variance $\mathcal{O}(1)$ for each instance. Repetition can be used to reduce the variance below what is required.

2. L-ancilla qubit measurement processes

Often, we want to compute the expectation value of an operator O of the form

$$O=\sum_{i=1}^{M} a_i U_i^\dagger V_i, \tag{3.10}$$

where U_i and V_i are unitary operators, a_i are real positive numbers ($a_i\geqslant 0$), and M is an integer power of 2. (In the case that M is less than a power of 2, we can complete this definition by setting $a_{M+1},\ldots,a_{M'}=0$, where M' is an integer power of 2.) We can compute this expectation value by preparing M different circuits, each one with one-ancilla qubit, and for each circuit measure $\langle U_i^\dagger V_i\rangle$ (see Sec. III C 1). Then, we multiply each result by the constant a_i and sum the results. However, in most cases, the preparation of the initial state is very difficult. This difficulty, however, can be reduced by using another way to measure this quantity that requires only one circuit.

We first write the operator O as

$$O=\mathcal{N}\sum_{i=1}^{M} \alpha_i^2 U_i^\dagger V_i, \tag{3.11}$$

where $\mathcal{N}=\Sigma_{i=1}^M a_i$ and $\alpha_i^2=a_i/\mathcal{N}$ ($\Sigma_{i=1}^M\alpha_i^2=1$). Then we construct a quantum circuit with the following steps.

(1) Prepare the state $|\Psi_0\rangle$ such that $\langle\Psi_0|O\Psi_0\rangle$ is the expectation value to be computed.

(2) Adjoin L ancillas to the initial state, where $L=J+1$ and $2^J=M$. The first of these ancillas, a_1, is prepared in the state $|+\rangle=(|0\rangle+|1\rangle)/\sqrt{2}$. This is done by applying the Hadamard gate to the initial state $|0\rangle$ [see Fig. 4(a)]. The other ancillas $\{a_2,a_3,\cdots,a_L\}$ are kept in the state $|0\rangle$.

(3) Apply a unitary evolution $E(\alpha_1,\alpha_2,\cdots,\alpha_M)$ to the ancillas $\{a_2,a_3,\cdots,a_L\}$ to obtain

$$|\psi\rangle=\alpha_1|00\cdots0\rangle+\alpha_2|00\cdots1\rangle+\cdots+\alpha_M|11\cdots1\rangle$$
$$=\sum_{i=1}^{M}\alpha_i|i\rangle,$$

where $|i\rangle$ is a tensorial product of the states ($|0\rangle$ or $|1\rangle$) of each ancilla: $|i\rangle=|\eta\rangle_{a_2}\otimes\cdots\otimes|\eta\rangle_{a_L}$, where η can be 0 or 1. The index i orders the orthonormal basis $|i\rangle$.

(4) Apply the controlled unitary operations $\tilde{U}_i$, which evolve the system by U_i if the state of the ancillas is $|0\rangle_{a_1}|i\rangle$. Then apply the controlled unitary operations $\tilde{V}_i$, which evolve the system by V_i if the state of the ancillas is $|1\rangle_{a_1}|i\rangle$. Once these evolution steps are finished, the state of the whole system is

$$|\Psi\rangle=\frac{1}{\sqrt{2}}\left[|0\rangle_{a_1}\sum_{i=1}^{M}\alpha_i|i\rangle U_i+|1\rangle_{a_1}\sum_{i=1}^{M}\alpha_i|i\rangle V_i\right]\otimes|\Psi_0\rangle.$$

(5) Measure the expectation value of $2\sigma_+^{a_1}=\sigma_x^{a_1}+i\sigma_y^{a_1}=2|0\rangle_{a_1}\langle 1|$. It is easy to see that it corresponds to the expectation value of the operator $\Sigma_{i=1}^M\alpha_i^2U_i^\dagger V_i$.

(6) Obtain the expectation value of O by multiplying $\langle 2\sigma_+^{a_1}\rangle$ by the constant $\mathcal{N}$.

The quantum circuit for this procedure is given in Fig. 10.

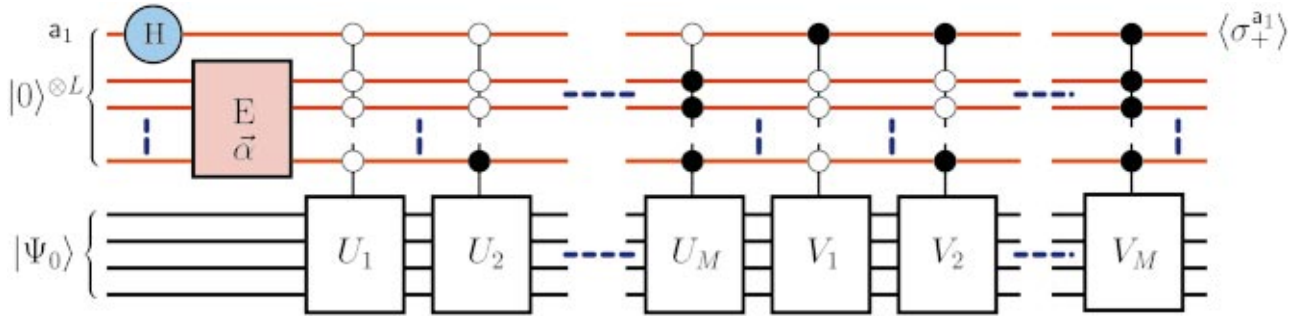

FIG. 10. (Color) Measurement of physical quantities using L-ancillas qubits $\{a_1,\ldots,a_L\}$. In this case $\langle\sigma_+^{a_1}\rangle=(1/2\mathcal{N})\langle\Psi_0|[\Sigma_{i=1}^M a_iU_i^\dagger V_i]|\Psi_0\rangle$ (see text).

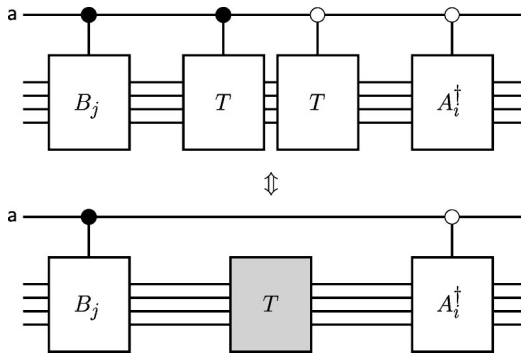

FIG. 11. Circuit for the measurement of spatial and time correlation functions. In this case $\langle 2\sigma_+^a\rangle=\langle T^\dagger A_i T B_j\rangle$. Notice the simplification achieved by reducing two controlled-T operations into only one uncontrolled-T operation.

3. Measurement of correlation functions

We now consider measuring correlation functions of the form $C_{AB}=\langle T^\dagger ATB\rangle$, where T is a unitary operator and A and B are operators that are expressible as a sum of unitary operators,

$$A=\sum_i \tilde{\alpha}_i A_i \quad \text{and} \quad B=\sum_j \tilde{\beta}_j B_j . \tag{3.12}$$

The operator T is fixed by the type of correlation function that we want to evaluate. In the case of dynamical correlation functions, T is e^{-iHt}, where H is the Hamiltonian of the system. For spatial correlation functions, T is the space translation operator $e^{-ip\cdot x}$ (p and x are configuration-space operators). The method for measuring these correlation functions is the same method described in Sec. III C 1 or Sec. III C 2. We can use either the one- or the L-ancilla measurement process.

To minimize the number of controlled operations and also the quantity of elementary gates involved, we choose $U_i^\dagger = T^\dagger A_i$ and $V_j = TB_j$. Now, we have to compute $\langle U_i^\dagger V_j\rangle$. In Fig. 11 we show the circuit for measuring this quantity, where the circuit has only one ancilla in the state $|+\rangle = (|0\rangle+|1\rangle)/\sqrt{2}$. There, the controlled operations were reduced by noting that the operation of T controlled on the state $|0\rangle$ of the ancilla followed by the operation of T controlled on the state $|1\rangle$ results in a no-controlled T operation. This is a very useful algorithmic simplification.

4. Measurement of the spectrum of an Hermitian operator

Many times one is interested in determining the spectrum of an observable (Hermitian operator) $\hat{Q}$, a particular case being the Hamiltonian H. Techniques for getting spectral information can be based on the quantum Fourier transform [22,23] and can be applied to physical problems [24]. For our purposes, the methods of the previous sections yield much simpler measurements without loss of spectral information. For a given H, the most common type of measurement is the computation of its eigenvalues or at least its lowest eigenvalue (the ground-state energy). To do this we start from a state $|\phi\rangle$ that has a nonzero overlap with the eigenstates of H. (For example, if we want to compute the energy of the ground state, then $|\phi\rangle$ has to have a nonzero overlap with the ground state.) For finite systems, $|\phi\rangle$ can be the solution of a mean-field theory (a Slater determinant in the case of fermions or Perelomov-Gilmore coherent states in the general case). Once we prepare this state (Sec. III A and Appendix A), we compute $\langle\hat{U}(t)\rangle=\langle\phi|\hat{U}(t)\phi\rangle$, where $\hat{U}$ is the evolution operator $\hat{U}(t)=e^{-iHt}$. We then note that

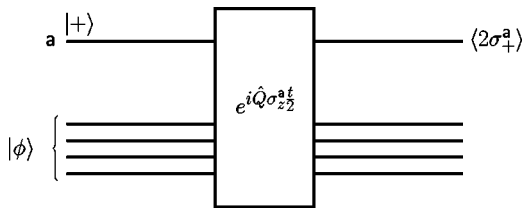

FIG. 12. Circuit for the measurement of the spectrum of an Hermitian operator $\hat{Q}$. In this case $\langle 2\sigma_+^a\rangle=\langle\phi|e^{-i\hat{Q}t}\phi\rangle$ (see text).

$$|\phi\rangle=\sum_{n=0}^{\mathcal{L}} \gamma_n|\Psi_n\rangle, \tag{3.13}$$

with $|\Psi_n\rangle$ eigenstates of the Hamiltonian H. Consequently

$$\langle\hat{U}(t)\rangle=\sum_{n=0}^{\mathcal{L}} |\gamma_n|^2 e^{-i\lambda_n t}, \tag{3.14}$$

where λ_n are the eigenvalues of H. The measurement of $\langle\hat{U}(t)\rangle$ is easily done by the steps described in Sec. III C 1 (setting $V=\hat{U}(t)$ and $U=\mathbb{1}$ in Fig. 9). Once we have this expectation value, we perform a classical fast Fourier transform [i.e., $\tilde{F}(\lambda)=\int\langle\hat{U}(t)\rangle e^{i\lambda t}dt$] and obtain the eigenvalues λ_n (see Appendix B),

$$\tilde{F}(\lambda)=\sum_{n=0}^{\mathcal{L}} 2\pi|\gamma_n|^2\delta(\lambda-\lambda_n). \tag{3.15}$$

Although we explained the method for the eigenvalues of H, the extension to any observable $\hat{Q}$ is straightforward, taking $\hat{U}(t)=e^{-i\hat{Q}t}$ and proceeding in the same way.

Two comments are in order. The first refers to an algorithmic optimization and points to decreasing the number of controlled operations (i.e., the number of elementary gates implemented). If we set $V=e^{-i\hat{Q}t}, U^\dagger=\mathbb{1}$ (see Fig. 9) and perform the type of measurement described in Sec. III C 1 the network has total evolution (ancilla plus system) $e^{-i\hat{Q}t/2}e^{i\hat{Q}\sigma_z^a t/2}$, while if we set $V=U^\dagger=e^{-i\hat{Q}t/2}$ the total evolution is $e^{i\hat{Q}\sigma_z^a t/2}$. Thus, this last algorithm reduces the number of gates by the number of gates it takes to represent the operator $e^{-i\hat{Q}t/2}$. The circuit is shown in Fig. 12.

The second comment refers to the complexity of the quantum algorithm as measured by system size. In general, it is difficult to find a state whose overlap scales polynomially with system size. If one chooses a mean-field solution as the initial state, then the overlap decreases exponentially with the system size; this is a ''signal problem,'' which also arises

in probabilistic classical simulations of quantum systems. The argument goes as follows: If $|\phi\rangle$ is a mean-field state for an N^d (=volume) system size whose (modulus of the) overlap with the true eigenstate is $|\gamma|<1$, and assuming that the typical correlation length of the problem ξ is smaller than the linear dimension N, if we double N, the new overlap is $\sim e^{2^d \ln|\gamma|}$.

We would like to mention that a well-known alternative way of computing part of the spectrum of an Hermitian operator is using the adiabatic connection according to the Gell-Mann-Low theorem, an approach that has been described in [1].

5. Mixed and exact estimators

We have already explained how to compute different types of correlation functions. But in most cases, we do not know the state whose correlations we want to obtain. The most common case is wanting the correlations in the ground state $|\Psi_0\rangle$ of some Hamiltonian H. Obtaining the ground state is a very difficult task; however, there are some useful methods to approximate these correlation functions.

Suppose we are interested in the mean value of a unitary operator $O(t)$. If we can prepare the initial state $|\Psi_T\rangle$ in such a way that $|\Psi_0\rangle=|\Psi_T\rangle+\epsilon|\Phi\rangle$ (ϵ is intended to be small), then after some algebraic manipulations [25], we have

$$\frac{\langle\Psi_0|O(t)|\Psi_T\rangle}{\langle\Psi_0|\Psi_T\rangle}=\frac{1}{2}\left[\frac{\langle\Psi_0|O(t)|\Psi_0\rangle}{\langle\Psi_0|\Psi_0\rangle}+\frac{\langle\Psi_T|O(t)|\Psi_T\rangle}{\langle\Psi_T|\Psi_T\rangle}\right]+\mathcal{O}(\epsilon^2), \tag{3.16}$$

where the term on the left-hand side of Eq. (3.16) is known as the ''mixed estimator.'' Also, we can calculate the second term on the right-hand side of Eq. (3.16) with an efficient quantum algorithm, since we are able to prepare easily $|\Psi_T\rangle$. Next, we show how to determine the mixed estimator using a quantum algorithm.

If $|\Psi_0\rangle$ is the ground state, then it is an eigenstate of the evolution operator $\hat{U}(t')=e^{-iHt'}$, and we can obtain the mixed estimator by measuring the mean value of $\hat{U}(t')O(t)$: Because $|\Psi_T\rangle=\Sigma_n a_n|\Psi_n\rangle$, where $a_n=\langle\Psi_n|\Psi_T\rangle$ and $|\Psi_n\rangle$ are the eigenstates of H [$\hat{U}(t')|\Psi_n\rangle=e^{-i\lambda_n t'}|\Psi_n\rangle$] we can measure (Sec. III C 3)

$$\langle\Psi_T|\hat{U}(t')O(t)|\Psi_T\rangle=\sum_n e^{i\lambda_n t'}\langle\Psi_T|\Psi_n\rangle\langle\Psi_n|O(t)|\Psi_T\rangle. \tag{3.17}$$

By performing a Fourier transform in the variable t' [$\tilde{F}(\omega)=\int e^{i\omega t'}F(t')dt'$] in Eq. (3.17) and making the relation between the expectation value for time t and the expectation value for $O(t)=\mathbb{1}$, we obtain the value of the mixed estimator. Then, by using Eq. (3.16), we obtain $\langle\Psi_0|O(t)|\Psi_0\rangle/\langle\Psi_0|\Psi_0\rangle$ up to order ϵ^2.

By similar steps, we can obtain expectation values of the form $\langle\Psi_n|O(t)|\Psi_{n'}\rangle/\langle\Psi_n|\Psi_{n'}\rangle$ for all n and n'. The trick consists of measuring (Sec. III C 3) the mean value of the operator $\hat{U}(t')O(t)\hat{U}^\dagger(t'')$ in the state $|\Psi_T\rangle$,

$$\langle\Psi_T|\hat{U}(t')O(t)\hat{U}^\dagger(t'')|\Psi_T\rangle=\sum_{n,n'} e^{i\lambda_n t'}e^{i\lambda_{n'}t''}\langle\Psi_T|\Psi_n\rangle\times\langle\Psi_{n'}|\Psi_T\rangle\langle\Psi_n|O(t)|\Psi_{n'}\rangle, \tag{3.18}$$

and then by performing a double Fourier transform in the variables t' and t'' [$\tilde{F}(\lambda,\lambda')=\int e^{i\lambda t'}e^{i\lambda' t''}F(t',t'')dt'dt''$] we obtain the desired results. A particular case of this procedure is the direct computation of the exact estimator $\langle\Psi_n|O(t)|\Psi_n\rangle/\langle\Psi_n|\Psi_n\rangle$.

IV. APPLICATION TO FERMIONIC LATTICE SYSTEMS

In this section, we illustrate a procedure for simulating fermionic systems on a quantum computer, showing as a particular example how to obtain the energy spectrum of the Hubbard Hamiltonian for a finite-sized system. We will obtain this spectrum through a simulation of a quantum computer on a classical computer, that is, by a quantum simulator [26].

We start by noting that the spin-fermion connection described in Eqs. (2.10) and (2.11) implies that the number of qubits involved in a two-dimensional lattice is $L=2(N_x\times N_y)$ if one uses the standard model to simulate spin-1/2 fermions. Also, the number of states for an L-qubit system is 2^L. From this mapping, the first $N_x\times N_y$ qubits represent the states that have spin-up fermions, and the other qubits [$(N_x\times N_y+1)$ up to $2(N_x\times N_y)$], spin-down fermions. In other words, if we have a system of four sites and have a state $|\Psi\rangle$ with one electron with spin up at the first site and one electron with spin down at the third site, then this state in second quantization is $|\Psi\rangle=a^\dagger_{1;\uparrow}a^\dagger_{3;\downarrow}|v\rangle$, where the fermionic operator $a^\dagger_{j;\sigma}$ creates a fermion in site j with spin σ, and $|v\rangle$ is the state with no particles (vacuum state). In the standard model, this state corresponds to

$$|\Psi\rangle=\sigma^1_+\prod_{l=1}^{6}\sigma^l_z\sigma^7_+|\tilde{v}\rangle=|0\rangle\otimes|1\rangle\otimes|1\rangle\otimes|1\rangle\otimes|1\rangle\otimes|1\rangle\otimes|0\rangle\otimes|1\rangle\rightarrow|\uparrow\downarrow\downarrow\downarrow\downarrow\downarrow\uparrow\downarrow\rangle, \tag{4.1}$$

where $|\tilde{v}\rangle$ is the vacuum of the quantum spin 1/2, which we have chosen to be $|\downarrow\downarrow\downarrow\downarrow\downarrow\downarrow\downarrow\downarrow\rangle$.

To represent the L-qubit system on a classical computer, we can build a one-to-one mapping between the 2^L possible states and the bit representation of an integer I defined by

$$I=\sum_{i=1}^{L}[n(i)\times 2^{i-1}], \tag{4.2}$$

where $n(i)$ (occupancy) is 0 if the spin of the ith qubit is $|1\rangle$ ($\downarrow$), or 1 if the state is $|0\rangle$ ($\uparrow$). In this way, the state described in Eq. (4.1) maps to $I=65$. Because we are interested in obtaining some of the eigenvalues of the Hubbard

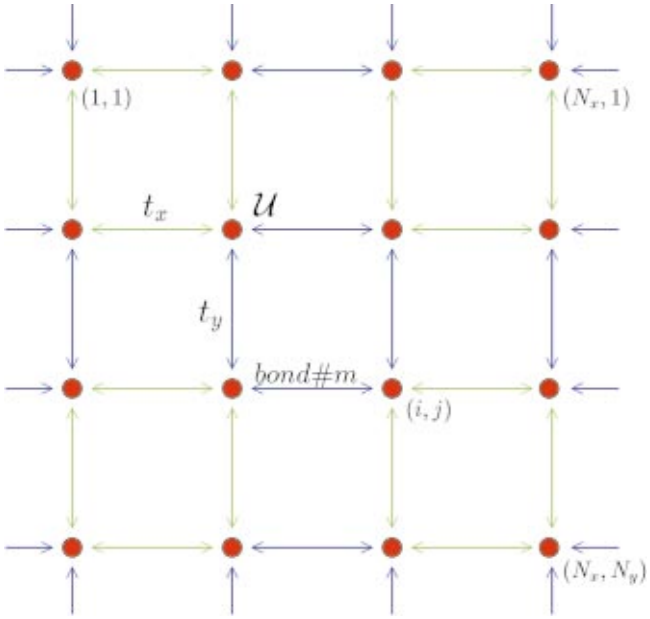

FIG. 13. (Color) Two-dimensional lattice in the Hubbard model. Here, the green and blue arrows identify the even and odd bonds.

model, we added an ancilla qubit (Fig. 12). The ''new'' system has $L=2(N_x\times N_y)+1$ qubits, and we can perform the mapping in the same way described above.

To simulate the evolution operator $\hat{U}(t)=e^{-iHt}$ on a classical computer using the above representation of quantum states, we programmed the ''elementary'' quantum gates of one- and two-qubit interactions. Each L-qubit state was represented by a linear combination of the integers I [Eq. (4.2)]. In this way, each unitary operation applied to one or two qubits modifies I by changing a bit. For example, if we flip the spin of the first qubit, the number I changes by 1.

We want to evaluate some eigenvalues of the spin-1/2 Hubbard model in two spatial dimensions. The model is defined on a rectangle of $N_x\times N_y$ sites and is parametrized by spin-preserving hoppings t_x and t_y between nearest-neighbor sites, and an interaction $\mathcal{U}$ on site between fermions of different z components of spin (Fig. 13). The Hamiltonian is

$$H=-\sum_{(i,j);\sigma}[t_x(a^{\dagger}_{(i,j);\sigma}a_{(i+1,j);\sigma}+a^{\dagger}_{(i+1,j);\sigma}a_{(i,j);\sigma}) + t_y(a^{\dagger}_{(i,j);\sigma}a_{(i,j+1);\sigma}+a^{\dagger}_{(i,j+1);\sigma}a_{(i,j);\sigma})] + \mathcal{U}\sum_{(i,j)} n_{(i,j);\uparrow}n_{(i,j);\downarrow}, \tag{4.3}$$

where $n_{(i,j);\sigma}=a^{\dagger}_{(i,j);\sigma}a_{(i,j);\sigma}$ is the number operator and the label $(i,j);\sigma$ identifies the site (X-Y position) and the z component of spin ($\sigma=\pm 1/2$). We assume that the fermionic operators satisfy strict periodic boundary conditions in both directions: $a_{(i,j);\sigma}=a_{(i+N_x,j);\sigma}=a_{(i,j+N_y);\sigma}$.

To obtain the energy spectrum for this model, we use the method described in Sec. III C 3 (See Fig. 12.) For this, we represent the system in the standard model, using the Jordan-Wigner transformation, mapping a two-dimensional spin-1/2 system into a one-dimensional chain, with the use of Eqs. (2.11) and (2.10) (Fig. 8).

As explained in Sec. III C 4, we find it convenient to start from the mean-field ground-state solution of the model, represented by H_{MF},

$$H_{MF}=-\sum_{(i,j);\sigma}[t_x(a^{\dagger}_{(i,j);\sigma}a_{(i+1,j);\sigma}+a^{\dagger}_{(i+1,j);\sigma}a_{(i,j);\sigma}) + t_y(a^{\dagger}_{(i,j);\sigma}a_{(i,j+1);\sigma}+a^{\dagger}_{(i,j+1);\sigma}a_{(i,j);\sigma})] + \mathcal{U}\sum_{(i,j)}[\langle n_{(i,j);\uparrow}\rangle n_{(i,j);\downarrow}+n_{(i,j);\uparrow}\langle n_{(i,j);\downarrow}\rangle-\langle n_{(i,j);\uparrow}\rangle\times\langle n_{(i,j);\downarrow}\rangle],$$

where the expressions in angular brackets are expectation values in the mean-field representation. Without loss of generality, we take $\mathcal{U}>0$ and select the antiferromagnetic ground-state mean-field solution. For this solution, we require N_x and N_y to be even numbers. If we were to simulate a one-dimensional lattice, we would, however, choose one of these numbers to be even and the other equal to 1. In the following we will only consider the half-filled case, which corresponds to having one fermion per site; i.e., $N_e=N_x\times N_y$.

First, we prepare the initial state. As discussed in Sec. III A, we do this by exploiting Thouless's theorem. We also use the first-order Trotter approximation (Sec. III B) and then decompose each term of the evolution into one- and two-qubit interactions. Here, the matrix M now depends on the parameters of the Hamiltonian, as does the ground-state mean-field solution. After the decomposition, we then prepare the desired initial state by applying the unitary evolutions to a boot-up (polarized) state. (See Appendix A.)

Next, we execute the evolution $\hat{U}(t)=e^{-iHt}$. For the sake of clarity we only present the first-order Trotter decomposition. To this end, we rewrote the Hubbard Hamiltonian as

$$H=K+V=K_{\uparrow}+K_{\downarrow}+V, \tag{4.4}$$

where K_{σ} is the kinetic term (hopping elements with spin σ) and V is the potential-energy term. Because $[K_{\sigma},V]_{-}\neq 0$ and $[K_{\uparrow},K_{\downarrow}]_{-}=0$ we approximated the short-time evolution operator $\hat{U}(\Delta t)$ by

$$\hat{U}(\Delta t)=e^{-iH\Delta t}\approx e^{-iK\Delta t}e^{-iV\Delta t}\quad(\Delta t\to 0). \tag{4.5}$$

Because the term $V=\mathcal{U}\Sigma_{(i,j)}n_{(i,j);\uparrow}n_{(i,j);\downarrow}=\Sigma_{l=1}^{N_x\times N_y}V_l$ is a sum of operators local to each lattice site, each of these terms commute so

$$e^{-iV\Delta t}=\prod_l e^{-iV_l\Delta t}. \tag{4.6}$$

The kinetic term is a sum over the bonds in the lattice (Fig. 13): $K_{\sigma}=\Sigma_{bonds}K_{bond;\sigma}$. Each bond joins two nearest-neighbor sites, either in the vertical or horizontal direction (Fig. 13). Because of the periodic boundary conditions, the

sites at the boundary of the lattice are also connected by bonds. We note that the terms in K that share a lattice site do not commute. For these terms we rewrite K_σ as

$$K_\sigma = K^o_{x;\sigma} + K^e_{x;\sigma} + K^o_{y;\sigma} + K^e_{y;\sigma}, \tag{4.7}$$

where $K^{e(o)}_{\mu;\sigma}$ are the kinetic terms (for spin σ) in the μ direction that involve the even (e) and odd (o) bonds in this direction (green and blue lines in Fig. 13). Then we perform the first-order Trotter approximation

$$e^{-iK_\sigma \Delta t} \approx e^{-iK^o_{x;\sigma}\Delta t} e^{-iK^e_{x;\sigma}\Delta t} e^{-iK^o_{y;\sigma}\Delta t} e^{-iK^e_{y;\sigma}\Delta t}. \tag{4.8}$$

Because the odd and even bonds are not connected, each term in Eq. (4.7) is a sum of terms that commute with each other, that is, $K^{e(o)}_{\mu;\sigma} = \Sigma_m K^{e(o);m}_{\mu;\sigma}$, where $[K^{e(o);m}_{\mu;\sigma}, K^{e(o);m'}_{\mu;\sigma}]_- = 0$, then

$$\exp(-iK^{e(o)}_{\mu;\sigma}\Delta t) = \prod_m \exp(-iK^{e(o);m}_{\mu;\sigma}\Delta t). \tag{4.9}$$

In summary we approximated the short-time evolution $\hat{U}(\Delta t)$ by

$$\begin{aligned}\hat{U}(\Delta t) \approx \Bigg[\prod_{m_1,m_2,m_3,m_4;\sigma} & \exp(-iK^{o;m_1}_{x;\sigma}\Delta t) \\ & \times \exp(-iK^{e;m_2}_{x;\sigma}\Delta t) \exp(-iK^{o;m_3}_{y;\sigma}\Delta t) \\ & \times \exp(-iK^{e;m_4}_{y;\sigma}\Delta t) \Bigg] \Bigg[\prod_l e^{-iV_l \Delta t} \Bigg].\end{aligned} \tag{4.10}$$

The total evolution operator is

$$\hat{U}(t) = \prod_j \hat{U}(\Delta t). \tag{4.11}$$

Each unitary factor in the evolution is easily decomposed into one- and two-qubit interactions (Sec. II B).

The final step is the measurement process. To obtain some of the eigenvalues, we use the circuit described in Fig. 12. Thus we are interested in the operator $\hat{U}(t')^{-\sigma^a_z}$ instead of $\hat{U}(t')$ so we actually performed the first two steps after adding an ancilla qubit a (Fig. 12), and then started with a "new" Hamiltonian $\tilde{H} = -H \otimes \sigma^a_z/2$ (and also a "new" evolution $\tilde{U}(t) = e^{-i\tilde{H}t}$), and performed the same steps described above.

The results for the simulation of the Hubbard model are shown in Fig. 14 (the eigenvalues were obtained using the correction of Appendix B). There, we also show the parameters Δt_1 and Δt_2 corresponding to the time steps we used in the initial state preparation and in the time evolution, where we used a first-order Trotter approximation.

In closing this section we emphasize that the simulation of the Hubbard model by a quantum computer, which uses the standard model of quantum computing is just an example. If instead one wants to simulate the Anderson model [27] using the same model of a quantum computer, then steps similar to those described above would be followed. (There are two types of fermions but the isomorphism still applies.) Similarly, if one wants to use a different quantum computer, which has another natural "language" (i.e., a different operator algebra, which therefore represents a different model of computation), the ideas developed above would be applied after simply choosing the right isomorphism or "dictionary" [3].

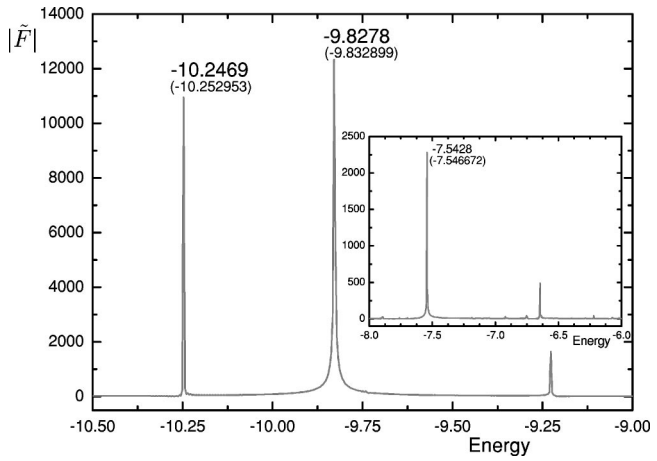

FIG. 14. Energy spectrum of the Hubbard model obtained from the quantum simulator. The lattice has 4×2 sites (which requires 16 qubits), with $t_x = 1$, $t_y = 1$, and $\mathcal{U} = 4$ and the time steps used in the Trotter approximation (to prepare the initial state and apply the evolution) are $\Delta t_1 = \Delta t_2 = 0.05$. The numbers in parentheses are results obtained from the Lanczos diagonalization.

V. CONCLUDING REMARKS

We addressed several broad issues associated with the simulation of physical phenomena by quantum networks. We first noted that in quantum mechanics the physical systems we want to simulate are expressed by operators satisfying certain algebras that may differ from the operators and the algebras associated with the physical system representing the quantum network used to do the simulation. We pointed out that rigorous mappings [3] between these two sets of operators exist and are sufficient to establish the equivalence of the different physical models to a universal model of quantum computation and the equivalence of different physical systems to that model.

We also remarked that these mappings are insufficient for establishing the fact that the quantum network can simulate any physical system efficiently even if the mappings between the systems only involves a polynomial number of steps. We argued that one must also demonstrate the main steps of initialization, evolution, and measurement, all of which scale polynomially with complexity. More is needed than just having a large Hilbert space and inherent parallelism. Further, we noted that some types of measurements important to understanding physical phenomena lack effective quantum algorithms.

In this paper we mainly explored various issues associated with efficient physical simulations by a quantum network, focusing on the construction of quantum-network models for

such computations. The main questions we addressed were how do we reduce the number of qubits and quantum gates needed for the simulation and how do we increase the amount of measurable physical information. We first summarized the quantum-network representation of the standard model of quantum computation, discussing both one-qubit and multiqubit circuits, and then recalled the connection between the spin and fermion representations. We next discussed the initialization, evolution, and measurement processes. In each case we defined procedures simpler than those presented in our previous paper [1], greatly improving the efficiency with which they can be done. We also gave algorithms that greatly expanded the types of measurements now possible. For example, besides certain correlation functions, the spectrum of operators, including the energy operator, is now possible. Our application of this technology to a system of lattice fermions and the construction of a simulator was also discussed and used the Hubbard model as an example. This application gave an explicit example of how the mapping between the operator of the physical system of interest and those of the standard model of quantum computation work. We also gave details of how we implemented the initialization, evolution, and measurement steps of the quantum network on a classical computer, thereby creating a quantum-network simulator.

Clearly, a number of challenges for the efficient simulation of physical systems on a quantum network remain. We are prioritizing our research on those issues associated with problems that are extremely difficult for quantum many-body scientists to solve on classical computers. There are no known efficient quantum algorithms for broad spectrum ground-state (zero-temperature) and thermodynamics (finite-temperature) measurements of correlations in quantum states. These measurements would help establish the phases of those states. Generating those states is itself a difficult task.

Another issue that is important for both classical and quantum simulations of physical phenomena concerns the discretization of continuous systems, that is, those that are characterized by an algebra of operators that admits an infinite-dimensional representation. On both classical and quantum computers this requires approximate representations on a finite-dimensional Hilbert space. The techniques that have been developed and are described in the extensive literature on classical simulations of quantum mechanics are directly applicable to simulations on quantum computers as has been noted by several authors [24,28,29]. An example is the simulation of interacting electrons in Euclidean $\mathbb{R}^d$ space. In such a case one can proceed similarly to the usual practice in classical simulations, i.e., discretize the system in a convenient fashion and simulate its lattice version. The type of discretization (single-particle basis) is system and observable dependent. For example, to simulate the homogeneous electron gas (jellium model) using a discrete quantum computer, one should first write its Hamiltonian in second-quantized form in a plane-wave basis (momentum representation) [30] and then study the convergence of the measured observable as a function of the momentum cutoff. However, for some densities ρ of the electron gas, it may be more convenient (from a convergence viewpoint) to use a different basis: for a diluted gas (small ρ) it might be more convenient to use a localized basis set (Wannier functions [31]). More esoteric basis-set choices, such as wavelets [32], are always possible.

Finally, many problems in physics simulation, such as the challenging protein-folding problem, are considered to be well modeled by classical physics. Can quantum-networks be used to obtain significantly better (more efficient) algorithms for such essentially classical-physics problems?

ACKNOWLEDGMENT

We thank Ivar Martin for useful discussions on the classical Fourier transform.

APPENDIX A: DIFFERENT STATE PREPARATION

1. Coherent state preparation: An example

Here we illustrate by example the decomposition of an operator of the form $e^{i\vec{a}^\dagger M\vec{a}}$ to generate an initial state. Typically M is generated by some mean-field solution to the physical problem of interest. Considerable detail is given.

We consider two spinless fermions in a one-dimensional lattice of four sites ($N_e=2, n=4$). The operators a_j and $a_j^\dagger$ annihilate and create a fermion in the site j of the lattice. We want to prepare an initial state $|\phi'\rangle = c_0^\dagger c_{\pi/2}^\dagger |v\rangle$ from the state $|\phi\rangle = a_1^\dagger a_2^\dagger |v\rangle$, where the operators c_k and $c_k^\dagger$ annihilate and create a fermion in the state of wave vector k, that is,

$$c_k^\dagger = \frac{1}{2}\sum_{j=1}^{4} e^{ikx_j} a_j^\dagger , \tag{A1}$$

where $k=0,\pi/2,\pi,3\pi/2$ are all possible wave vectors of the system and x_j is the position in the lattice of the site (i.e., $x_j=j-1$).

From Eq. (A1), we see that the state $|\phi'\rangle$ is a linear combination of states of the form $a_i^\dagger a_j^\dagger |v\rangle$. The change of basis e^{iM} (Eq. 3.5) between the two sets of fermionic operators is

$$\begin{pmatrix} c_0^\dagger \\ c_{\pi/2}^\dagger \\ c_\pi^\dagger \\ c_{3\pi/2}^\dagger \end{pmatrix} = \frac{1}{2}\begin{pmatrix} 1 & 1 & 1 & 1 \\ 1 & i & -1 & -i \\ 1 & -1 & 1 & -1 \\ 1 & -i & -1 & i \end{pmatrix} \begin{pmatrix} a_1^\dagger \\ a_2^\dagger \\ a_3^\dagger \\ a_4^\dagger \end{pmatrix}. \tag{A2}$$

If we calculate the eigenvalues and the eigenvectors of the matrix e^{iM}, from Eq. (A2) we obtain

$$e^{iM_D} = \begin{pmatrix} -1 & 0 & 0 & 0 \\ 0 & i & 0 & 0 \\ 0 & 0 & 1 & 0 \\ 0 & 0 & 0 & 1 \end{pmatrix}, \tag{A3}$$

where M_D is M in its diagonal form. Then, we have

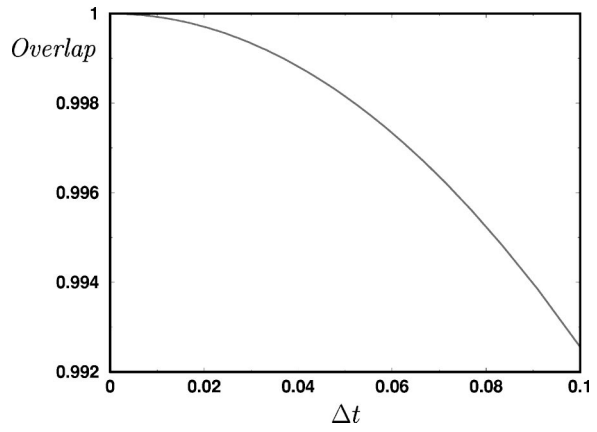

FIG. 15. Overlap between the exact initial state and the state prepared with the Trotter decomposition for a system with two fermions in a four-site lattice.

$$M_D = -i \ln(e^{iM_D}) = \begin{pmatrix} \pi & 0 & 0 & 0 \\ 0 & \pi/2 & 0 & 0 \\ 0 & 0 & 0 & 0 \\ 0 & 0 & 0 & 0 \end{pmatrix}. \tag{A4}$$

To obtain the matrix $M = A^\dagger M_D A$, we need to know the unitary matrix A, which is constructed with the eigenvectors of the matrix e^{iM}. In this case we have

$$A^\dagger = \begin{pmatrix} -1/2 & 0 & 1/\sqrt{2} & 1/\sqrt{2} \\ 1/2 & -1/\sqrt{2} & 1/\sqrt{2} & 0 \\ 1/2 & 0 & -1/\sqrt{2} & 1/\sqrt{2} \\ 1/2 & 1/\sqrt{2} & 1/\sqrt{2} & 0 \end{pmatrix}, \tag{A5}$$

hence, the Hermitian matrix M is

$$M = \frac{\pi}{4} \begin{pmatrix} 1 & -1 & -1 & -1 \\ -1 & 2 & 1 & 0 \\ -1 & 1 & 1 & 1 \\ -1 & 0 & 1 & 2 \end{pmatrix}. \tag{A6}$$

In order to obtain $|\phi'\rangle$ we prepare the state $|\phi\rangle$ and then apply the evolution $U = e^{i\vec{a}^\dagger M \vec{a}}$. If we want to simulate this fermionic system in a quantum computer (standard model), we have to use the spin-fermion connection (Sec. II C) and write the operator U as a combination of single-qubit rotations and two-qubit interactions. Also, the initial state $|\phi\rangle$ must be written in the standard model,

$$|\phi\rangle = a_1^\dagger a_2^\dagger |v\rangle = \sigma_+^1(-\sigma_z^1 \sigma_+^2)|\tilde{v}\rangle = \sigma_+^1 \sigma_+^2 |\tilde{v}\rangle \tag{A7}$$

$$= |0\rangle_1 \otimes |0\rangle_2 \otimes |1\rangle_3 \otimes |1\rangle_4 = |\uparrow\uparrow\downarrow\downarrow\rangle, \tag{A8}$$

where the vacuum state in the standard model is $|\tilde{v}\rangle = |1\rangle_1 \otimes |1\rangle_2 \otimes \cdots \otimes |1\rangle_n = |\downarrow\downarrow\cdots\downarrow\rangle$ $[(\Pi_{l=1}^{j-1} - \sigma_z^l)\sigma_-^j |\tilde{v}\rangle = a_j |v\rangle = 0]$. With this mapping, the state $|\phi'\rangle$ is a linear combination of states of the z component of spin 0.

As noted in Sec. III B, sometimes the decomposition of the operator U in terms of one- and two-qubit operations is very difficult. To avoid this problem, we can use the Trotter decomposition (3.7). In Fig. 15 we show the overlap (projection) between the state $|\phi'\rangle$ and the state prepared using the first-order Trotter decomposition of U applied to the state $|\phi\rangle$.

2. Jastrow-type wave functions

A Jastrow-type wave function is often a better approximation to the actual state of an interacting system, particularly when interactions are strong and short ranged. Often one varies the parameters in these functions to produce a state that satisfies a variational principle for some physical quantity like the energy. Such states build in correlated many-body effects and are, in general, entangled states. The states described in Sec. 1 of Appendix A) are unentangled.

The classic form of a Jastrow-type wave function for fermions is [18]

$$|\Psi_0\rangle = e^S |\phi'\rangle, \tag{A9}$$

where $S = \Sigma_{ij} \alpha_{ij} c_i^\dagger c_j + \Sigma_{ijkl} \beta_{ijkl} c_i^\dagger c_j^\dagger c_k c_l + \cdots$ is an operator that creates particle and hole excitations, and $|\phi'\rangle$ is typically a Slater determinant. The N-body correlations embodied in S take into account the short-range forces not included in $|\phi'\rangle$. We will assume that α_{ij} and β_{ijkl} have been determined by some suitable means (for example, by a coupled-cluster calculation). If we decompose e^S into a linear combination of unitary operators, we can then decompose $|\Psi_0\rangle$ into a linear combination of Slater determinants and thus prepare $|\Psi_0\rangle$ as explained in [1]. Also, if the coefficients α_{ij} and β_{ijkl} are small, we can approximate e^S by the first few terms in its Taylor expansion. Again, the state $|\Psi_0\rangle$ will be a linear combination of Slater determinants.

Obviously, it is more natural for a quantum computer to generate a correlated state of the form

$$|\Psi_0\rangle = e^{iS} |\phi'\rangle, \tag{A10}$$

where e^{iS} is a unitary operator. In order to determine the N-body correlation coefficients α_{ij} and β_{ijkl}, one could, in principle, use the technique of unitary transformations introduced by Villars [33].

APPENDIX B: DISCRETE FOURIER TRANSFORMS

In practice, to evaluate the discrete fast Fourier transform (DFFT) one uses discrete samples, therefore Eq. (3.15) must be modified accordingly. In Fig. 14 we see that instead of having δ functions (Dirac's functions), we have finite peaks in some range of energies, close to the eigenvalues of the Hamiltonian. Accordingly, one cannot determine the eigenvalues with the same accuracy as other numerical calculations. However, there are some methods that give the results more accurately than the DFFT.

As a function of the frequency Ω_m, the DFFT $[\tilde{F}(\Omega_m)]$ is given by

$$\tilde{F}(\Omega_m)=\Delta t\sum_{j=0}^{N-1} F(t_j)e^{i\Omega_m t_j}, \tag{B1}$$

where $t_j=j\Delta t$ are the different times at which the function F is sampled [in the case of Sec. III C 4, $F(t_j)=\langle\hat{U}(t_j)\rangle$], $\Omega_m=2\pi m/N\Delta t$ are the possible frequencies to evaluate the FFT of $F(t)$ and N is the number of samples. (N must be an integer power of 2.)

Since we are interested in $F(t)=\Sigma_{n=0}^{\mathcal{L}}|\gamma_n|^2e^{-i\lambda_n t}$ (Eq. 3.14),

$$\tilde{F}(\Omega_m)=\Delta t\sum_{n=0}^{\mathcal{L}}|\gamma_n|^2\sum_{j=0}^{N-1} e^{i[\Omega_m-\lambda_n]t_j}, \tag{B2}$$

and then

$$\tilde{F}(\Omega_m)=\Delta t\sum_{n=0}^{\mathcal{L}}|\gamma_n|^2\frac{e^{i(\Omega_m-\lambda_n)\Delta tN}-1}{e^{i(\Omega_m-\lambda_n)\Delta t}-1}. \tag{B3}$$

If Ω_m is close to one of the eigenvalues λ_n and the λ_n are sufficiently far apart to be well resolved, we can neglect all terms in the sum other than n. If we take Ω_m and $\Omega_{m+1}=\Omega_m+2\pi/N\Delta t$, both close to λ_n in such a way that $|\tilde{F}(\Omega_m)|,|\tilde{F}(\Omega_{m+1})|\gg 0$, then from Eq. (B3) we find that

$$\frac{\tilde{F}(\Omega_{m+1})}{\tilde{F}(\Omega_m)}\approx\frac{e^{i(\Omega_m-\lambda_n)\Delta t}-1}{e^{i(\Omega_{m+1}-\lambda_n)\Delta t}-1}. \tag{B4}$$

After simple algebraic manipulations [and approximating $e^{i(\Omega_m-\lambda_n)\Delta t}\approx 1+i(\Omega_m-\lambda_n)\Delta t$ and the same for the denominator in Eq. (B4)] we obtain the correction to the energy λ_n,

$$\lambda_n=\Omega_m+\Delta\lambda_n \tag{B5}$$

with

$$\Delta\lambda_n\approx-\frac{2\pi}{N\Delta t}\mathrm{Re}\left[\frac{\tilde{F}(\Omega_{m+1})}{\tilde{F}(\Omega_m)-\tilde{F}(\Omega_{m+1})}\right]. \tag{B6}$$

[1] G. Ortiz, J.E. Gubernatis, E. Knill, and R. Laflamme, Phys. Rev. A **64**, 22319 (2001).

[2] S. Somaroo, C.-H. Tseng, T.F. Havel, R. Laflamme, and D.G. Cory, Phys. Rev. Lett. **82**, 5318 (1999).

[3] C.D. Batista and G. Ortiz, Phys. Rev. Lett. **86**, 1082 (2001), and unpublished results.

[4] We are aware of at least one case where the sign problem can be mapped onto an NP (nondeterministic polynomial) -complete problem. This is the 3-SAT (satisfiability) problem [5]. Therefore, one cannot yet claim that a quantum computer can solve ''all'' sign problems, otherwise one would claim that one is solving all NP-complete problems and this has not been rigorously established.

[5] E. Farhi, J. Goldstone, S. Gutmann, J. Lapan, A. Lundgren, and D. Preda, Science **292**, 472 (2001).

[6] B.M. Terhal and D.P. DiVincenzo, Phys. Rev. A **61**, 022301 (2000).

[7] Because of our recent work [1], the restriction to fermions allows some reduction in background presentation. However, our discussion has obvious applications, for example, to the simulation of a system of hard-core bosons (or any other particle statistics or, in mathematical terms, any other operator algebra).

[8] $\mathbb{1}=\begin{pmatrix}1&0\\0&1\end{pmatrix}$, $\sigma_x=\begin{pmatrix}0&1\\1&0\end{pmatrix}$, $\sigma_y=\begin{pmatrix}0&-i\\i&0\end{pmatrix}$, $\sigma_z=\begin{pmatrix}1&0\\0&-1\end{pmatrix}$.

In this particular representation, the states $|0\rangle$ and $|1\rangle$ are the vectors

$$|0\rangle=\begin{pmatrix}1\\0\end{pmatrix}\ \text{and}\ |1\rangle=\begin{pmatrix}0\\1\end{pmatrix},$$

and the Bloch sphere (Fig. 2) provides a convenient three-dimensional real space representation of the single-qubit state $|a\rangle$, which can be parametrized as $|a\rangle=\cos(\theta/2)|0\rangle+e^{i\varphi}\sin(\theta/2)|1\rangle$.

[9] A. Barenco *et al.*, Phys. Rev. A **52**, 3457 (1995).

[10] D. DiVincenzo, Phys. Rev. A **51**, 1015 (1995).

[11] Although here we use the algebra of the Pauli matrices (standard model), for a different model of computation we should change the set of elementary gates but the general methodology remains the same.

[12] M.D. Price, S.S. Somaroo, A.E. Dunlop, T.F. Havel, and D.G. Cory, Phys. Rev. A **60**, 2777 (1999).

[13] S.S. Somaroo, D.G. Cory, and T.F. Havel, Phys. Lett. A **240**, 1 (1998).

[14] S. Bravyi and A. Kitaev, e-print quant-ph/0003137.

[15] P. Jordan and E. Wigner, Z. Phys. **47**, 631 (1928).

[16] E. Fradkin, Phys. Rev. Lett. **63**, 322 (1989).

[17] L. Huerta and J. Zanelli, Phys. Rev. Lett. **71**, 3622 (1993).

[18] J.-P. Blaizot and G. Ripka, *Quantum Theory of Finite Systems* (MIT Press, Cambridge, 1986).

[19] A. Perelomov, *Generalized Coherent States and their Applications* (Springer-Verlag, Berlin, 1986).

[20] For a brief review, see M. Suzuki, in *Quantum Monte Carlo Methods in Condensed-Matter Physics*, edited by M. Suzuki (World Scientific, Singapore, 1993), p. 1.

[21] C. Miquel, J.P. Paz, M. Saraceno, E. Knill, R. Laflamme, and C. Negrevergne (unpublished).

[22] A. Yu Kitaev, e-print quant-ph/9511026.

[23] R. Cleve, A. Ekert, C. Macchiavello, and M. Mosca, Proc. R. Soc. London, Ser. A **454**, 339 (1998).

[24] D.S. Abrams and S. Lloyd, Phys. Rev. Lett. **83**, 5162 (1999).

[25] J.W. Negele and H. Orland, *Quantum Many-Particle Systems* (Addison-Wesley, Redwood City, 1988).

[26] Our quantum simulator can handle up to 20 qubits.

[27] See, for instance, J. Bonča and J.E. Gubernatis, Phys. Rev. B **58**, 6992 (1998).

[28] S. Wiesner, e-print quant-ph/9603028.
[29] C. Zalka, Proc. R. Soc. London, Ser. A **454**, 313 (1998).
[30] A.L. Fetter and J.D. Walecka, *Quantum Theory of Many-Particle Systems* (McGraw-Hill, Boston, 1971).
[31] J. Callaway, *Quantum Theory of the Solid State* (Academic Press, San Diego, 1991).
[32] T.A. Arias, Rev. Mod. Phys. **71**, 267 (1999).
[33] F. Villars, in *Nuclear Physics*, Proceedings of the International School of Physics ''Enrico Fermi,'' Course XXIII, edited by V. F. Weisskopf (Academic Press, New York, 1963), p. 1.